UM-SCC-103: a tongue cancer cell line established from a pregnant woman that recapitulates the tumorigenic stem cell population of the primary tumor

John Henry Owen, **Samantha J. Davis**, **Alice L. Tang**, **Martin P. Graham**, **Michael J. Czerwinski**, **Marcella Kaddoura**, **Silvana Papagerakis**, **Carol R. Bradford**, **Thomas E. Carey**, and **Mark E.P. Prince**
Department of Otolaryngology/Head & Neck Surgery, University of Michigan, Ann Arbor, MI

Abstract

Immortalized cell lines are useful tools for studying the diversity of primary tumors. A highly aggressive HNSCC of the oral cavity was diagnosed in a twenty-six-year-old pregnant woman with a low risk factor profile. Cells from the primary tumor were passaged in culture and genotyped as a unique cell line, UM-SCC-103. Cell populations were sorted for CD44 expression, ALDH activity and Bmi-1 gene expression to assess the cancer stem cell compartments. The primary tumor and cell line contained 19.03% and 19.62% CD44^{high} cells, respectively. CD44^{high} cancer stem cells from UM-SCC-103 formed tumors after flank injections in mice that reconstituted the overall heterogeneity of the primary tumor. CD44 staining and histology in the primary tumor and tumors grown *in vivo* from the cell line were similar. CD44^{high} cells sorted from the primary tumor resulted in lung colony formation in 2/2 tail vein injections in immunocompromised mice while CD44^{low} cells did not. Similarly, CD44^{high} cells from UM-SCC-103 formed lung tumors in 2/4 mice while CD44^{low} cells failed to do so. The similarity in marker expression and tumorigenic behavior between the primary tumor and the resulting cell line strongly suggests that the immortalized cell line resembles the primary tumor it was derived from and provides an important research tool to the study of head and neck squamous cell carcinomas in young patients.

Introduction

Established cell lines are just as diverse as the head and neck squamous cell carcinoma primary tumors from which they are derived. Acquiring a broad array of immortalized cell lines for research purposes is vital to study the variety of characteristics and behaviors of the tumors that these cell lines represent. The advantage of a replenishable supply of laboratory-cultivated cells for applications is especially important when samples from primary tumors are limited. The selective pressure of establishing a new cell line *in vitro* and whether it appropriately recapitulates the primary tumor has been noted[1–3]. Such concern is partially alleviated by the use of xenografts in animal models[4,5]. Direct comparisons between cells from the primary tumor and the cell line later established from the primary tumor in regards

Corresponding Author: Dr. Mark E. Prince, 1500 E. Medical Center Dr., 1903 Taubman Center, SPC 5312, Ann Arbor, MI 48109, Phone: (734) 647-6498, Fax: (734) 936-8052.

to biomarker expression and tumorigenic potential may further aid to draw the similarities between the two cell populations.

Tumorigenicity in cell lines has been described as the process by which neoplastic cells growing in tissue culture form tumors when inoculated into an animal[6,7]. Multiple xenograft models exist that provide for the observation of the tumorigenicity of a cancer cell line[8]. Subcutaneous injections along the flanks of an immunosuppressed animal can be used to demonstrate the potential of the cells to propagate *in vivo*[9]. Similarly, tail vein injection of a cell suspension can result in lung colonization if a tumorigenic cell population is used[10–12]. Lung colonization can be monitored over time by prior transduction of the cell line with a bioluminescent marker[13].

Cancer stem cells (CSC) are a subpopulation of cells that are highly tumorigenic, possess the capability to self-renew, and have the capacity to recreate the initial tumor heterogeneity[6]. CSC have been isolated before in HNSCC using the markers cluster of differentiation 44 (CD44) and aldehyde dehydrogenase (ALDH)[14,15]. CD44 is a transmembrane surface adhesion molecule containing a ligand-binding region for hyaluronan, whose signaling has been linked to tumor progression, invasion and metastasis in solid tumors, including HNSCC[16,17]. Our lab has also shown a compartment of CSC exists in HNSCC that has an increase of ALDH activity and is able to propagate *in vivo* when compared to cells with low ALDH activity[15].

Identification of the CSC compartment in primary tumors and cell lines is a necessary precursor to development of targeted therapy(s) that could be applied against this subpopulation in conjunction with more traditional cancer treatments. We describe a tumor that arose in the tongue of a pregnant woman, became highly aggressive, spread leading to distant metastasis, and death of a young woman. Head and neck squamous cancers are extremely rare in women and even more uncommon in pregnant women. This cell line provides a unique model to better understand the biological behavior of a rare aggressive tongue cancer arising in a young pregnant woman. The tumorigenicity of the primary tumor, as well as the resulting cell line established from it, can be attributed to the presence of an identifiable cancer stem cell population.

Materials and Methods

Approvals for the collection of cancer specimens and for use of the animal model were obtained through the appropriate review boards. The University of Michigan's Guide for the Care and Use of Laboratory Institutional Animals was followed.

Establishment of the cell line

Primary tumor tissue was transported from the operating room to the lab and was washed extensively in Earle's balanced salt solution containing penicillin, streptomycin, and amphotericin B. The tissue was then minced by scalpel blade and placed in culture flasks and covered with complete Dulbecco's Modified Eagle Medium (Gibco) containing 10% fetal bovine serum, L-glutamine, penicillin, streptomycin. 0.05% Trypsin-EDTA was used for partial trypsinization to aid in fibroblast removal. When sufficient outgrowth of epithelial

cells was observed, tumor cells were detached using 0.125% trypsin and plated into new culture flasks. Supernatants were tested for mycoplasma using Myco Alert Mycoplasma Testing Kit (Lonza).

Tumor digestion

Tumor tissue from the primary tumor, designated HN-111, and all xenografts were minced and digested in DMEM/F12 (Gibco) with 1X collagenase/hyaluronidase (Stem Cell Technologies). After two hours of digestion, the mixtures were strained through a 40 um sieve and the cells were counted before being prepared for flow cytometry.

Immunohistochemistry

UM-SCC-103 cells were cultured on chamber slides until 70% confluent at which point they were fixed and permeabilized with 4% paraformaldehyde and 0.1% Triton-x (Sigma). Tissue slides from the surgical specimen and from the murine xenografts were deparaffinized, rehydrated and peroxidase-quenched (DakoCytomation). All slides were incubated in Antigen Retrieval Solution (DakoCytomation) for 40 minutes in 92°C water bath with a buffer change midway and allowed to cool to room temperature for 20 minutes. Horse serum was used for blocking (30 minutes at room temperature). Primary antibody anti CD44 (BD Pharmingen) was added and allowed to incubate overnight at 4°C. Slides were washed and secondary antibodies linked to avidin/biotin peroxidase (ABC Kit; Vector Laboratories) were used to detect primary antibody binding.

RNA Extraction, Reverse Transcription Polymerase Chain Reaction, Gene Expression

RNA from UM-SCC-103 was isolated by an RNA mini kit (Qiagen). cDNA was synthesized using Reverse Transcription System Kit (Promega) according to the manufacturer's protocol and detection of Bmi-1 was done using the forward primer 5'-aggccaacagcccagcagga-3' and the reverse primer 5'-actgcactggagtactggggc-3'.

Luciferase Transduction

UM-SCC-103 was transduced with human immunodeficiency virus (HIV) with a luciferase reporter, a lentiviral vector containing a pLentiloxbackbone and a cytomegalovirus promoter. Polybrene was added to increase efficiency of the transduction. Successful gene delivery was confirmed via green fluorescent protein (GFP) visualization in a side-by-side transduction of the HIV-GFP vector under identical conditions.

Flow Cytometry

CD44 expression was detected using an APC-conjugated mouse antibody (BD Pharmingen). Cells were suspended in Hank's Balanced Salt Solution (HBSS; Gibco) with 2% Heat Inactivated Calf Serum (HICS) added to a concentration of 1 million cells per mL. Five uL of antibody was added per mL of cell suspension, and left to incubate on ice for 20 minutes. An APC-conjugated IgG2b isotype control antibody was used under the same conditions (BD Pharmingen). Aldehyde dehydrogenase (ALDH) expression was detected using the ALDEFLUOR kit (StemCell Technologies). Cells from UM-SCC-103 were brought to single cell suspension in Aldefluor Assay Buffer (AAB), and incubated with ALDH

substrate (BAAA, 5 mol/L per 1×10^6 cells) for 45 minutes at 37° C. Concurrently, diethylaminobenzaldehyde (DEAB 50 mmol/L) was added to a separate sample also containing BAAA for an ALDH-inhibited control. Samples were washed and resuspended in AAB. 4', 6-diamidino-2-phenylindole (DAPI; BD Pharmingen) was used as a cell viability indicator. Fluorescence-activated cell sorting gates were established using the inhibited control (DEAB) along the fluorescein isothiocyanate (FITC) channel with excitation and emission wavelengths of approximately 495 nm/521 nm. For CD44 expression, cell sorting gates were established using the APC-conjugated isotype control along the allophycocyanin (APC) channel with excitation and emission wavelengths of approximately 650 nm/660 nm.

Flank Injections

CD44^{high}/ALDH^{high} and CD44^{low}/ALDH^{low} fractions from UM-SCC-103 were collected into separate tubes and 30,000 cells from each fraction were suspended in a mixture of 100 uL of DMEM and 100 uL of Matrigel extracellular matrix (BD Biosciences). The resulting 200 uL volumes were injected subcutaneously into opposite flanks of NOD/SCID mice (Jackson Laboratories). Tumor growth from the CD44^{high}/ALDH^{high} injection was allowed to persist for 12 weeks until harvested for sectioning and digestion. CD44^{high} and CD44^{low} fractions from UM-SCC-103-Luc were collected into separate tubes and 10,000 cells from each fraction were injected into both flanks of NOD/SCID mice. Each mouse was injected with either the CD44^{high} fraction in both flanks or the CD44^{low} fraction in both flanks and imaged at 4 week intervals.

Tail Vein Injections

CD44^{high} and CD44^{low} fractions from UM-SCC-103-Luc were collected into separate tubes and cells from each fraction were suspended in 200 uL of phosphate-buffered saline (PBS, Gibco). The suspensions were injected into the tail veins of restrained NOD/SCID mice and imaged at 4 week intervals.

Bioluminescence Imaging

All animals treated with UM-SCC-103-Luc injections were imaged with the Xenogen IVIS-200 imaging system. Treated mice were given intraperitoneal injections of 100 uL luciferin at a concentration of 40 mg/mL and allowed to sit for 10 minutes before being anesthetized with isofluorane and imaged.

Results

Case Report

A 26-year-old woman presented with a growing painful lesion of the right lateral oral tongue. Evaluation revealed a moderately differentiated T4N2b squamous cell cancer of the oral tongue. She had a remote 6-pack-year history of smoking but no other risk factors. Notably, she had recently become pregnant. She chose to undergo elective termination of her pregnancy. Surgical resection including hemiglossectomy, bilateral neck dissections and a forearm free tissue reconstruction was performed. Due to the presence of multiple metastatic lymph nodes, several with extracapsular spread and extensive perineural invasion at the primary tumor site, she elected to undergo radiation with chemotherapy post-

operatively. After initially receiving 3 doses of taxol/platinum based chemotherapy and 5.4 gray of radiotherapy she was unable to come to her appointments and was lost to follow up. She presented about six months later with a large neck abscess that was proven to represent recurrent cancer that was found to be unresectable due to the extent of the neck disease. She completed a course of chemotherapy and radiation but developed distant metastasis and eventually succumbed to her disease.

Primary Tumor

The primary tumor, designated HN-111, had a CD44^{high} fraction consisting of 19.03% of the viable cancer cell population (Figure 1). These CD44^{high}cells developed lung colonies in 2/2 tail vein injections and a large abdominal tumor in one mouse (Table 1). There were no growths resulting from CD44^{low} injections. Histology and CD44 staining were similar between the primary tumor and the abdominal tumor resulting from the CD44^{high} injection (Figure 2). It was not possible to evaluate the primary tumor for ALDH expression due to the small amount of tissue available for analysis.

UM-SCC-103

Pieces of the primary tumor were grown in culture and established as UM-SCC-103 (Figure 3). At passage 23, UM-SCC-103 had a CD44^{high} fraction of 19.62%, and an ALDH^{high} fraction of 3.17% (Figure 4). CD44^{high}/ALDH^{high} cells grew flank tumors in 2/2 mice, while CD44^{low}/ALDH^{low} cells failed to form tumors in the flank (Figure 5). The flank tumor derived from the CD44^{high}/ALDH^{high} injection resembled UM-SCC-103 in CD44 staining and ALDH activity, with 4.12% of the population of viable cells from the tumor being ALDH^{high} (Figure 6). CD44^{high} cells expressed Bmi-1 to a greater extent than both unsorted and CD44^{low} cells. ALDH^{high} cells had a 2.84-fold increase in Bmi-1 gene expression over ALDH^{low} cells (Figure 7).

UM-SCC-103-Luc

Cells transduced with luciferase grew lung tumors in 2/4 mice receiving CD44^{high} tail vein injections and 0/4 mice receiving CD44^{low} injections in the tail vein. One each of 2 mice developed lung tumors at cell concentrations of 100,000 and 50,000 (Figure 8). The mouse with a lung tumor after 50,000 CD44^{high} cells was confirmed to have tumor by histology (Figure 9). Flank tumors developed in 4/4 injection sites with CD44^{high}/ALDH^{high} cells and only 2/4 injection sites with CD44^{low}/ALDH^{low} cells (Figure 10). The intensity of bioluminescence observed from the CD44^{high}/ALDH^{high} flank tumors also exceeded that of the CD44^{low}/ALDH^{low} flank growths by nearly ten-fold as measured by Total Flux (p/s) or Average Radiance (p/s/cm^2/sr) (Figure 11; Table 2).

Discussion

Cell lines have been critically important to investigators studying head and neck cancer and other malignant tumors. The development of a head and neck cell line from a piece of primary tumor is difficult and occurs with an efficiency of about 25%, requires a high degree of experience, and is very time and labor intensive[18–20]. Despite these difficulties it

is vital that we continue to develop new cell lines that represent the variety of primary cancers that occur in patients.

UM-SCC-103 represents a unique cell line that was derived from a tongue cancer that developed in a young woman who was pregnant at the time her cancer was diagnosed. Analysis of the resultant cancer cell line reveals that the cell line shares features with the primary tumor, suggesting it closely resembles the primary tumor. The tumorigenic stem cell population that exists in the primary tumor is conserved during its immortalization and can be identified with the same stem cell markers. The percentage of CD44^{high} cells remains relatively unchanged from primary tumor to cell line after over twenty passages. ALDH activity could not be measured in the primary tumor, but the stem cell population composed of ALDH^{high} cells remains similar in cultured cells when compared to a xenograft tumor grown from the stem cell population. The sorted ALDH^{high} cells are capable of reconstituting the original tumor heterogeneity, fulfilling a condition required of a cancer stem cell[6,21–24].

Similarly, *in vivo* tumorigenicity of the stem cell population in the cell line was also comparable to that of the primary tumor. CD44^{high} cells sorted from the primary tumor were able to grow nodules in the lungs of mice, which is also where CD44^{high} cells from the luciferase-transduced cell line were seen. In both the cell line and the cells sorted from the primary tumor, the CD44^{low} injections failed to grow tumors. The targeting of the lung epithelium by CD44 has been reported in other cancers as a potential marker of metastasis[25–29]. CD44^{high} cells that were also ALDH^{high} grew tumors in each attempted flank injection. These tumors also grew more quickly and were larger than the tumors from CD44^{low}/ALDH^{high} injections as measured through bioluminescence of the luciferase-transduced cell line. It is unknown whether those tumors arose from a sorting error or whether they propagated from a CD44^{low}/ALDH^{low} cancer stem cell. Current literature suggests the possibility of the cancer stem cell to move between different phenotypes, and this may be reflected in the expression of stem cell markers such as CD44 and ALDH[30,31].

Furthermore, evaluation of Bmi-1 expression, a gene shown to be expressed in stem cells[32,33], reveals a higher expression in the putative CSC population sorted from the cell line. This was observed in both the CD44^{high} and ALDH^{high} populations when compared with their respective low populations. Further research is warranted into how the CD44^{high}/ALDH^{high} population compares in gene expression, and whether utilizing both stem cell markers will narrow down the active stem cell population rather than using a single marker. While cell lines should not be viewed as a perfect mirror of the tumor, as it existed in the patient, this cell line does reflect the same tumorigenic behavior *in vivo* and should be regarded as a valuable tool to study the role of cancer stem cells in HNSCC progression. The patient had a stormy course with rapid progression. Her tumor also had a remarkably high stem cell population as measured by CD44 and ALDH high populations. It is not possible to determine whether this high fraction of cells with a cancer stem cell phenotype was responsible for the aggressive course of her tumor progression since she also had interruptions of her treatment which is also associated with poor response to treatment and tumor progression. UM-SCC-103 is available for other investigators to study.

Citations

1. Hughes P, Marshall D, Reid Y, et al. The costs of using unauthenticated, over-passaged cell lines: how much more data do we need? BioTechniques. 2007; 43:575–586. [PubMed: 18072586]

2. Dancik GM, Ru Y, Owens CR, et al. A framework to select clinically relevant cancer cell lines for investigation by establishing their molecular similarity with primary human cancers. Cancer Res. 2011; 71(24):7398–7409. [PubMed: 22012889]

3. Ertel A, Verghese A, Byers SW, et al. Pathway-specific differences between tumor cell lines and normal and tumor tissue cells. Molecular Cancer. 2006; 5:55. [PubMed: 17081305]

4. Kerbel RS. Human tumor xenografts as predictive preclinical models for anticancer drug activity in humans: better than commonly perceived- but they can be improved. Cancer BiolTher. 2003; 2(4):S134–S139.

5. Richmond A, Su Y. Mouse xenograft models vs GEM models for human cancer therapeutics. Dis Model Mech. 2008; 1(2–3):78–82. [PubMed: 19048064]

6. Reya T, Morrison SJ, Clarke MF, Weissman IL. Stem cells, cancer, and cancer stem cells. Nature. 2001; 414:105–111. [PubMed: 11689955]

7. Al-Hajj M, Wicha MS, Benito-Hernandez A, et al. Prospective identification of tumorigenic breast cancer cells. ProcNatlAcadSci USA. 2003; 100:3983–3988.

8. Fidler IJ. Rationale and methods for the use of nude mice to study the biology and therapy of human cancer metastasis. Cancer Metastasis Rev. 1986; 5(1):29–49. [PubMed: 2942306]

9. Wong RJ, Kim SH, Joe JK, et al. Effective treatment of head and neck squamous cell carcinoma by an oncolytic herpes simplex virus. Journal of the American College of Surgeons. 2009; 193(1):12–21. [PubMed: 11442249]

10. Elkin M, Vlodavsky I. Tail vein assay of cancer metastasis. Current Protocols in Cell Biology. 2001; 12:19.2.1–19.2.7.

11. Hu J, Verkman AS. Increased migration and metastatic potential of tumor cells expressing aquaporin water channels. Federation of American Societies for Experimental Biology Journal. 2006; 20(11):1892–1894. [PubMed: 16818469]

12. Davis SJ, Divi V, Owen JH, et al. Metastatic potential of cancer stem cells in head and neck squamous cell carcinoma. Arch Otolaryngol Head Neck Surg. 2010 Dec; 136(12):1260–1266. [PubMed: 21173377]

13. Nogowa M, Yuasua T, Kimura S, et al. Monitoring luciferase-labeled cancer cell growth and metastasis in different in vivo models. Cancer Letters. 2005; 217(2):243–253. [PubMed: 15617843]

14. Prince ME, Sivanandan R, Kaczorowski A, et al. Identification of a subpopulation of cells with cancer stem cell properties in head and neck squamous cell carcinoma. ProcNatlAcadSci U S A. 2007 Jan 16; 104(3):973–978.

15. Clay MR, Tabor M, Owen JH, et al. Single-marker identification of head and neck squamous cell carcinoma cancer stem cells with aldehyde dehydrogenase. Head and Neck. 2010; 32(9):1195–1201. [PubMed: 20073073]

16. Marhaba R, Zöller M. CD44 in cancer progression: adhesion, migration and growth regulation. J MolHistol. 2004 Mar; 35(3):211–231.

17. Sugahara KN, Hirata T, Hayasaka H, et al. Tumor cells enhance their own CD44 cleavage and motility by generating hyaluronan fragments. Journal of Biological Chemistry. 2006; 281(9):5861–5868. [PubMed: 16407205]

18. Lin CJ, Grandis JR, Carey TE, et al. Head and neck squamous cell carcinoma cell lines: established models and rationale for selection. Head and Neck. 2007; 29(2):163–188. [PubMed: 17312569]

19. Kim SY, Chu KC, Lee HR, et al. Establishment and characterization of nine new head and neck cancer cell lines. Acta Oto-Laryngologica. 1997; 117(5):775–784. [PubMed: 9349880]

20. White JS, Weissfeld JL, Ragin CCR, et al. The influence of clinical and demographic risk factors on the establishment of head and neck squamous cell carcinoma cell lines. Oral Oncology. 2007; 43(7):701–712. [PubMed: 17112776]

21. Jordan CT, Guzman ML, Noble M. Cancer stem cells. N Engl J Med. 2006; 355:1253–1261. [PubMed: 16990388]

22. Soltysova A, Altanerova V, Altaner C. Cancer stem cells. Neoplasma. 2005; 52(6):435–440. [PubMed: 16284686]

23. Guo W, Lasky JL, Wu H. Cancer stem cells. Pediatric Research. 2006; 59:59R–64R.

24. Zhou J, Zhang Y. Cancer stem cells. Cell Cycle. 2008; 7(10):1360–1370. [PubMed: 18418062]

25. Indinnimeo M, Cicchini C, Giarnieri E, et al. Evaluation of CD44 variant 6 expression and clinicopathological factors in pulmonary metastases from colon carcinoma. Oncol Rep. 2003; 10(6):1875–1877. [PubMed: 14534711]

26. Iwasaki A, Tashiro K, Kuwahara M, et al. Expression of variant CD44, exon 6 in patients with metastatic pulmonary tumor. Oncol Rep. 1997; 4(4):815–818. [PubMed: 21590147]

27. Shiratori H, Koshino T, Uesugi M, et al. Acceleration of lung metastasis by up-regulation of CD44 expression in osteosarcoma-derived cell transplanted mice. Cancer Letters. 2001; 170(2):177–182. [PubMed: 11463496]

28. Sheridan C, Kishimoto H, Fuchs RK, et al. CD44$^+$/CD24$^-$ breast cancer cells exhibit enhanced invasive properties: an early step necessary for metastasis. Breast Cancer Research. 2006; 8:R59. [PubMed: 17062128]

29. Seiter S, Arch R, Reber S, et al. Prevention of tumor metastasis formation by anti-variant CD44. J Exp Med. 1993; 177:443–455. [PubMed: 8426113]

30. Brabletz T, Hlubek F, Spaderna S, et al. Invasion and metastasis in colorectal cancer: epithelial-mesenchymal transition, mesenchymal-epithelial transition, stem cells and β-catenin. Cells Tissues Organs. 2005; 179:56–65. [PubMed: 15942193]

31. Biddle A, Liang X, Gammon L, et al. Cancer stem cells in squamous cell carcinoma switch between two distinct phenotypes that are preferentially migratory or proliferative. Cancer Res. 2011; 71(15):5317–5326. [PubMed: 21685475]

32. Al-Hajj M, Becker MW, Wicha M, et al. Therapeutic implications of cancer stem cells. Curr Opin Genet Dev. 2004; 14(1):43–47. [PubMed: 15108804]

33. Lessard J, Sauvageau G. Bmi-1 determines the proliferative capacity of normal and leukaemic stem cells. Nature. 2003; 423:257–260.
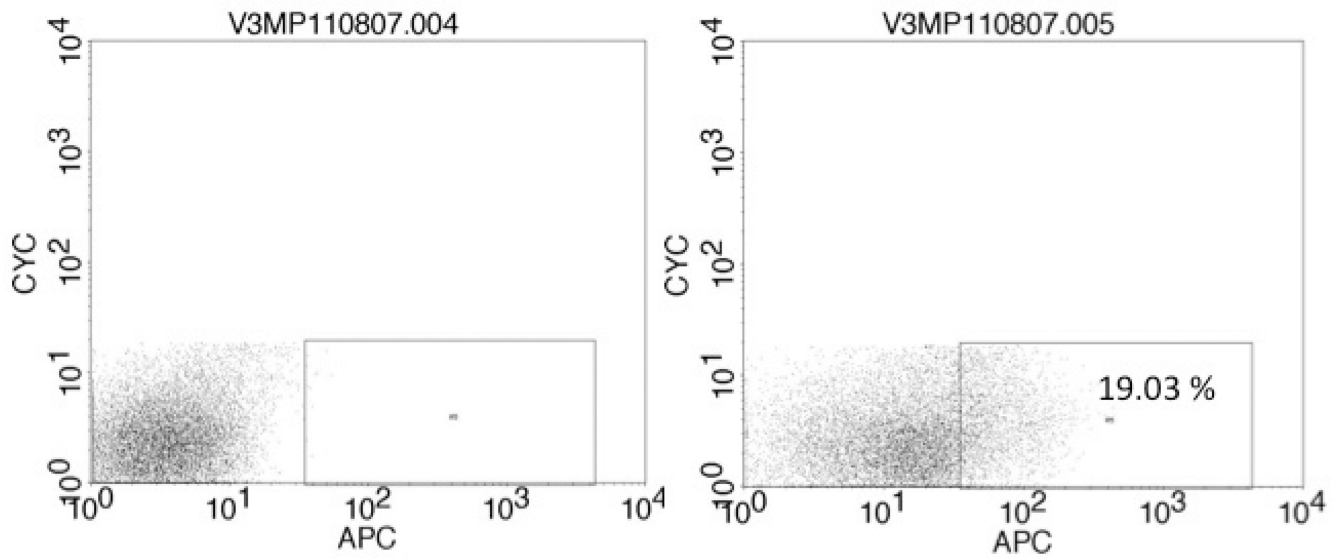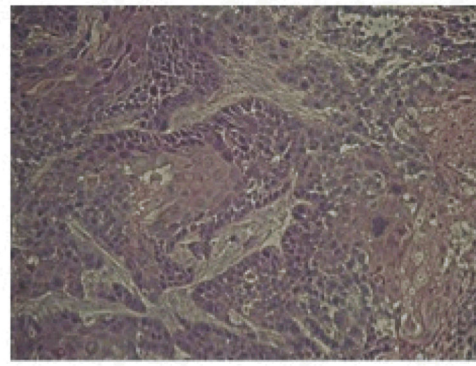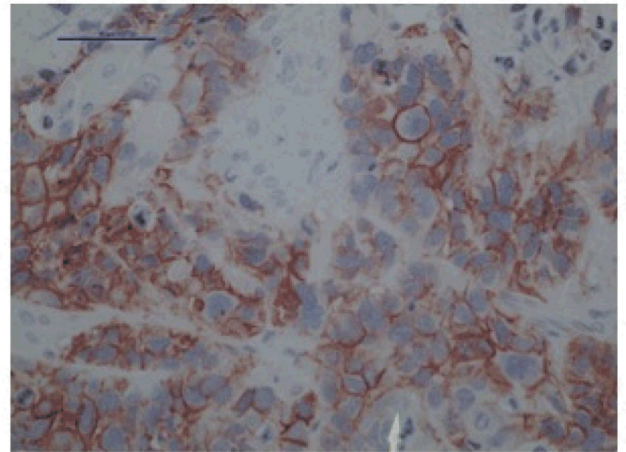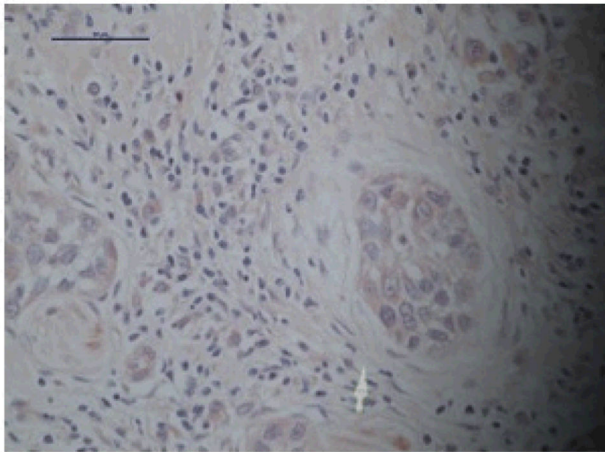
Figure 1.
Cells from HN-111 were stained with DAPI (left) or DAPI and the APC-conjugated CD44
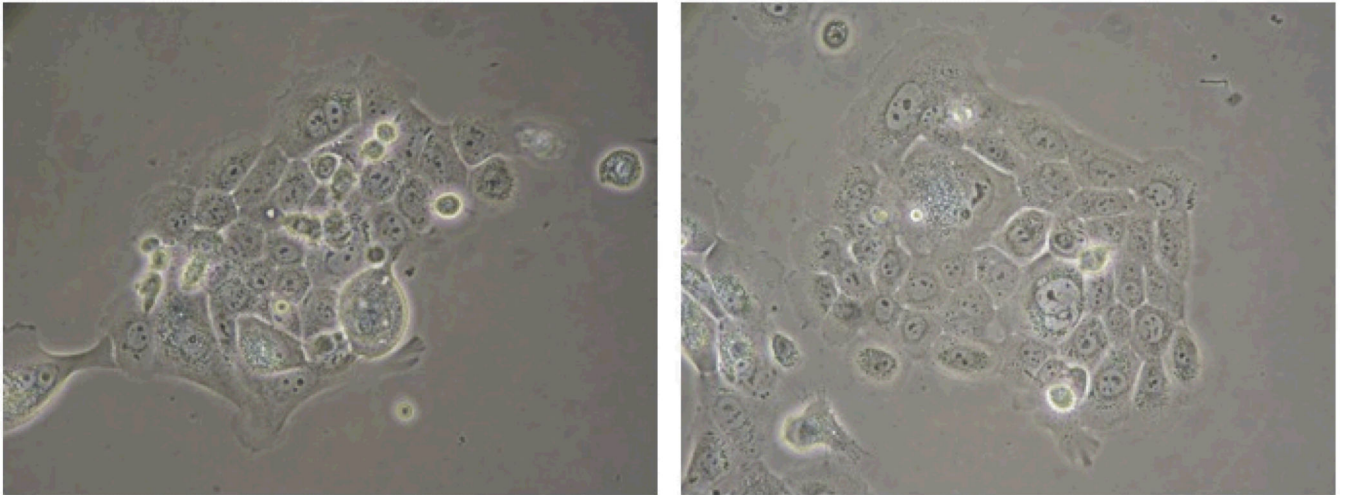antibody (right). Cells were collected for tail vein injections.
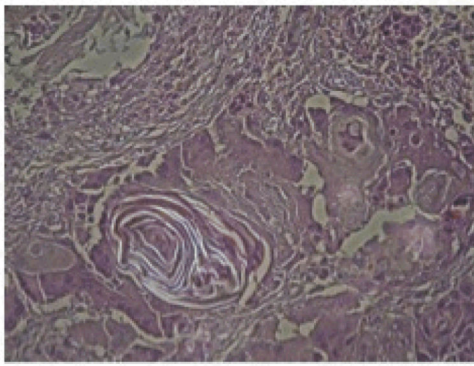
Figure 2.
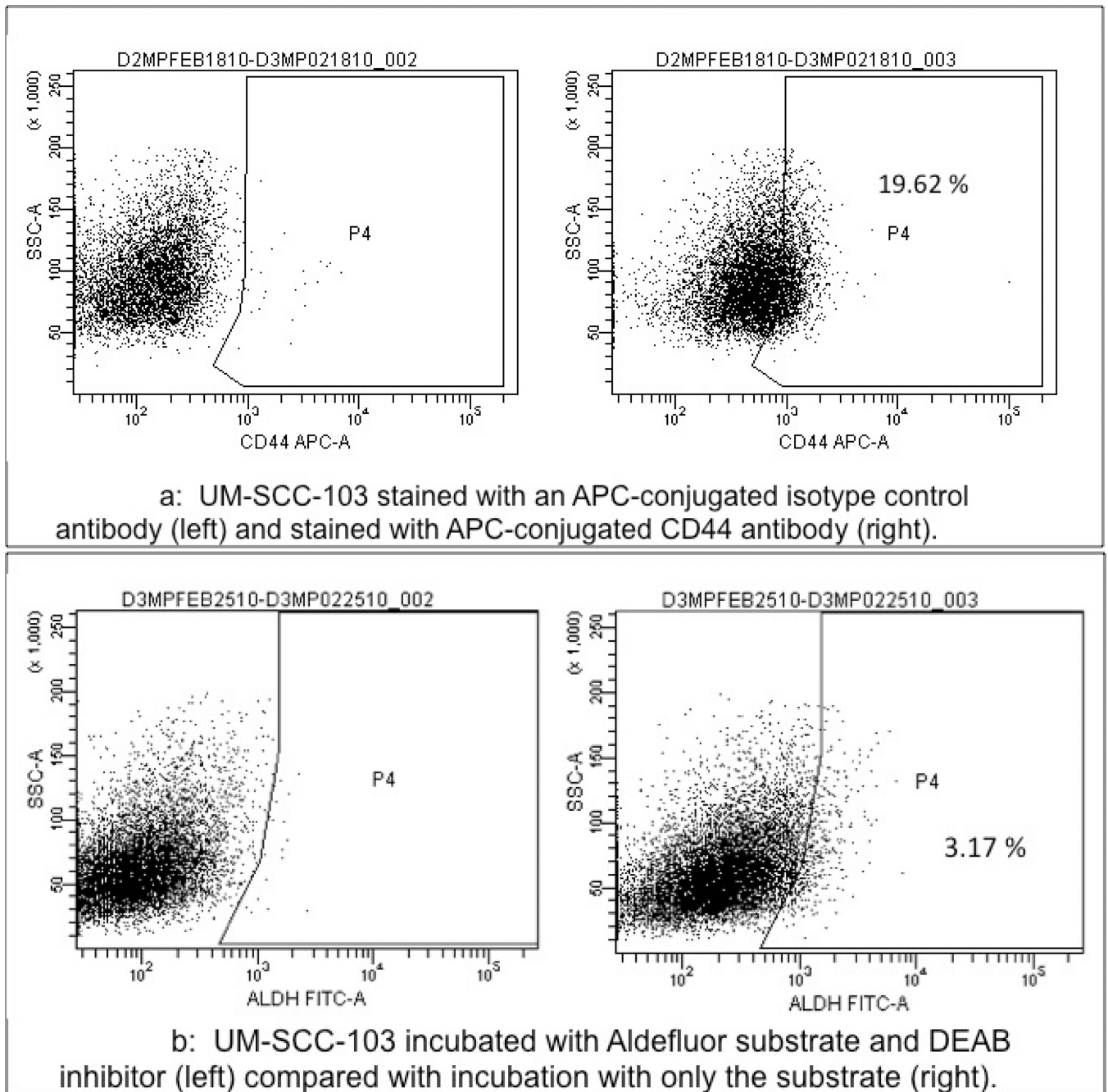H&E slides of the primary tumor (left) and the abdominal xenograft resulting from the CD44^{high} injection (right). Staining for CD44 was strong in both (bottom images).

Figure 3.
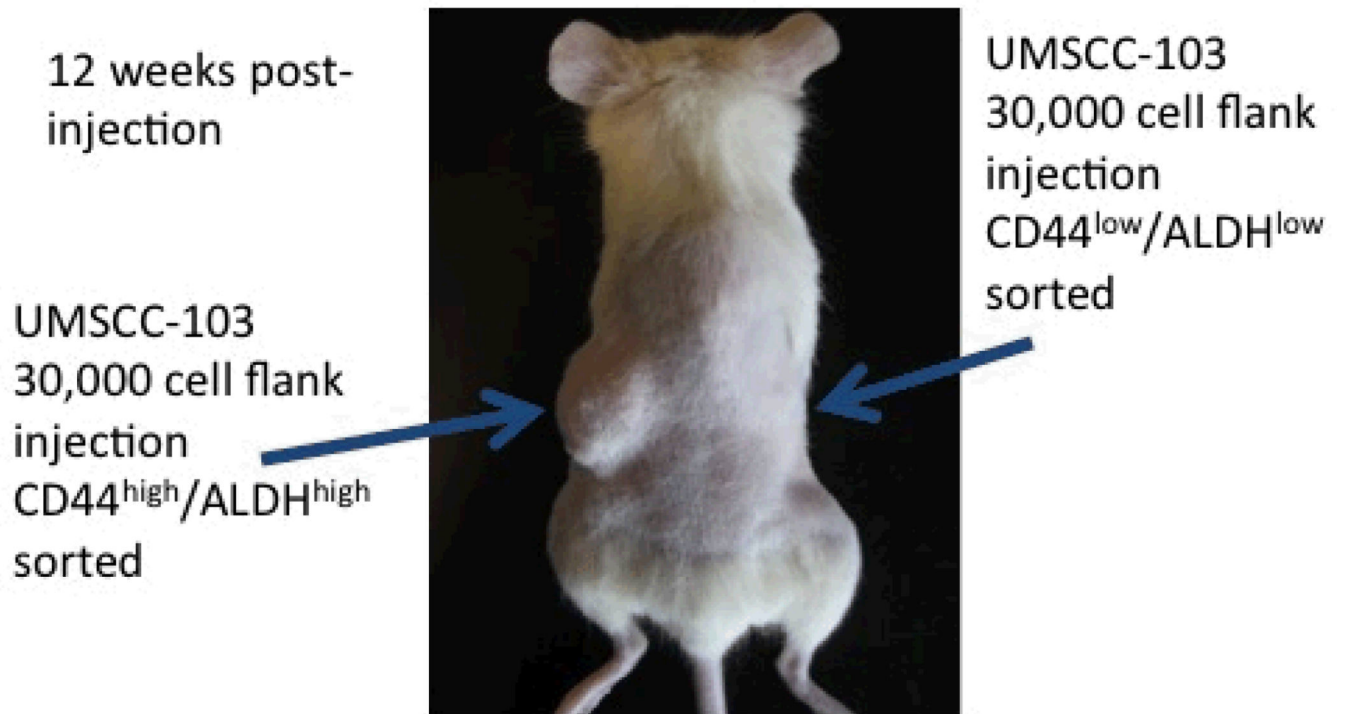UM-SCC-103 at passage 23. Cells from this passage were analyzed for CD44 and ALDH to compare with those from the primary HN-111.

a: UM-SCC-103 stained with an APC-conjugated isotype control antibody (left) and stained with APC-conjugated CD44 antibody (right).

b: UM-SCC-103 incubated with Aldefluor substrate and DEAB inhibitor (left) compared with incubation with only the substrate (right).
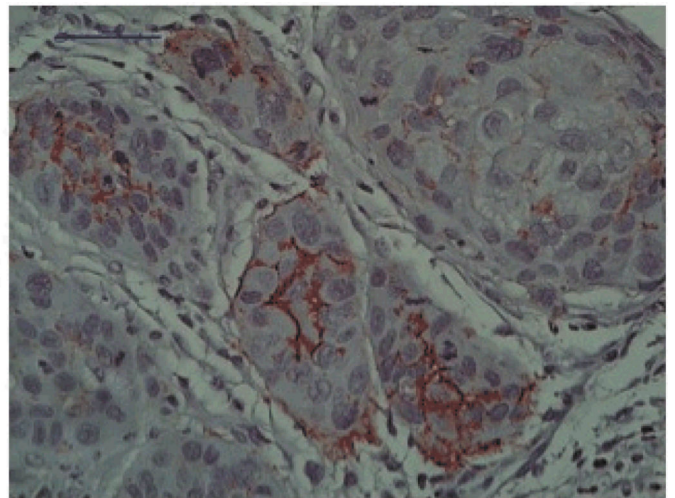
Figure 4.
a: UM-SCC-103 stained with an APC-conjugated isotype control antibody (left) and stained with APC-conjugated CD44 antibody (right).
b: UM-SCC-103 incubated with Aldefluor substrate and DEAB inhibitor (left) compared with incubation with only the substrate (right).

	CD44^{high}/ALDH^{high}	CD44^{low}/ALDH^{low}
Tumor Growth	2 out of 2 mice	0 out of 2 mice

12 weeks post-injection

UMSCC-103 30,000 cell flank injection CD44^{high}/ALDH^{high} sorted

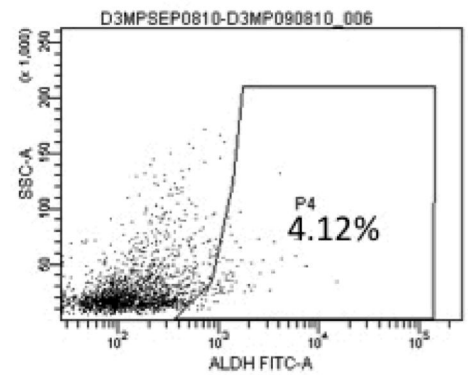UMSCC-103 30,000 cell flank injection CD44^{low}/ALDH^{low} sorted

Figure 5.
2/2 mice grew tumors on the left flank, corresponding with the cancer stem cell population.
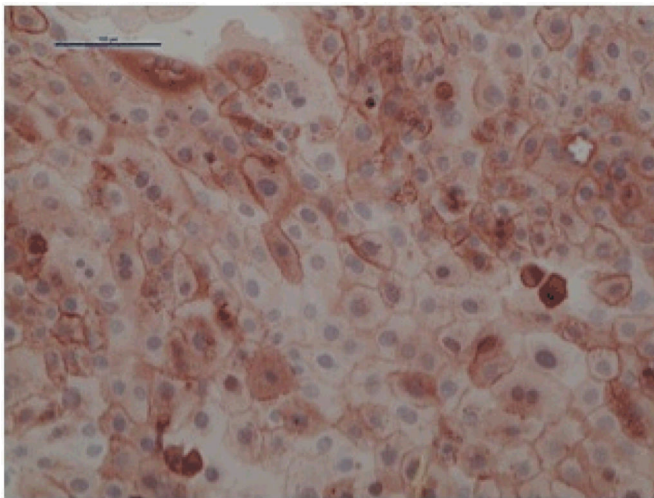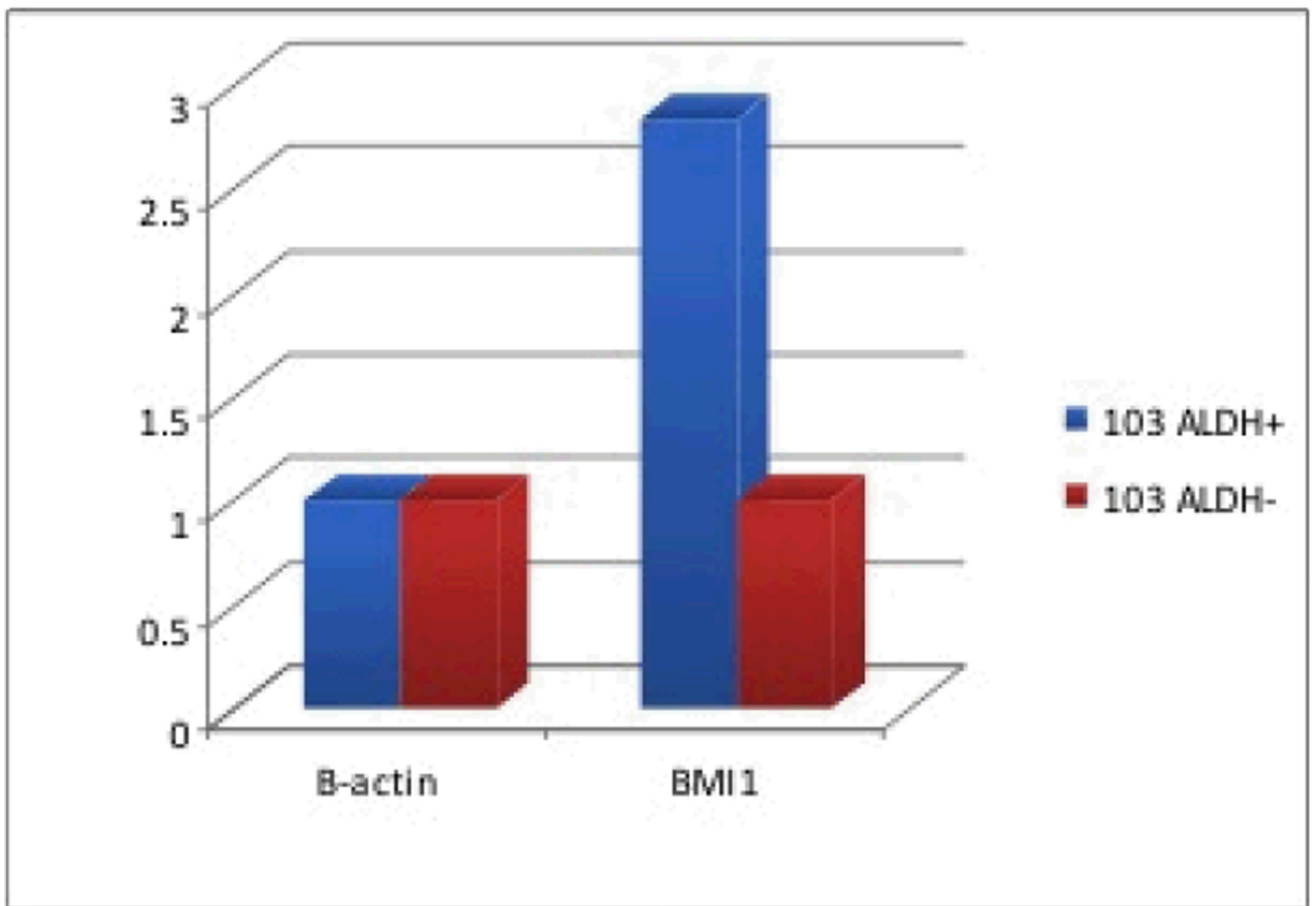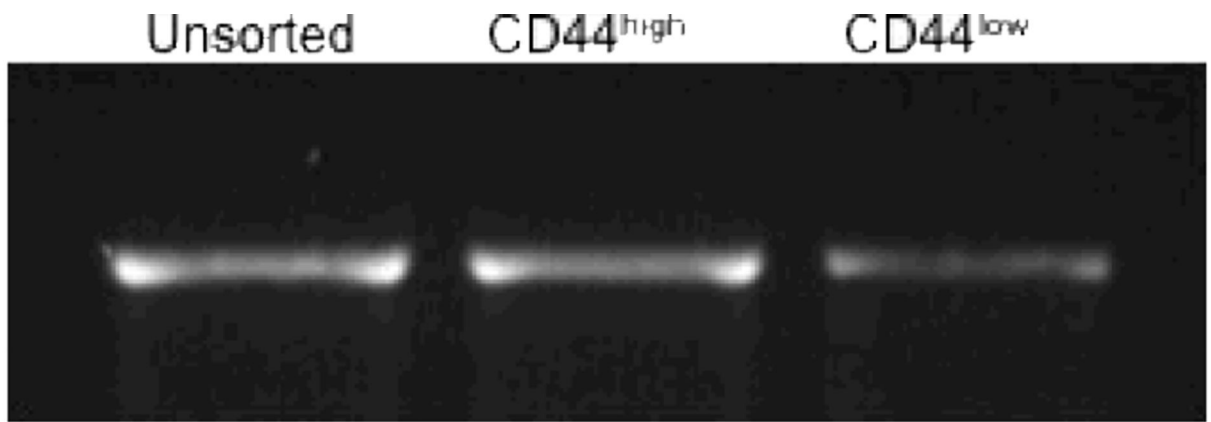
UM-SCC-103 stained for CD44

UM-SCC-103 Xenograft stained for CD44

Figure 6.
UM-SCC-103 cells in culture stained strongly for CD44 (top left). CD44 staining from the CD44high/ALDHhigh xenograft resembled the original primary (top right). The xenograft repopulated the ALDH activity of the unsorted cell line (right).
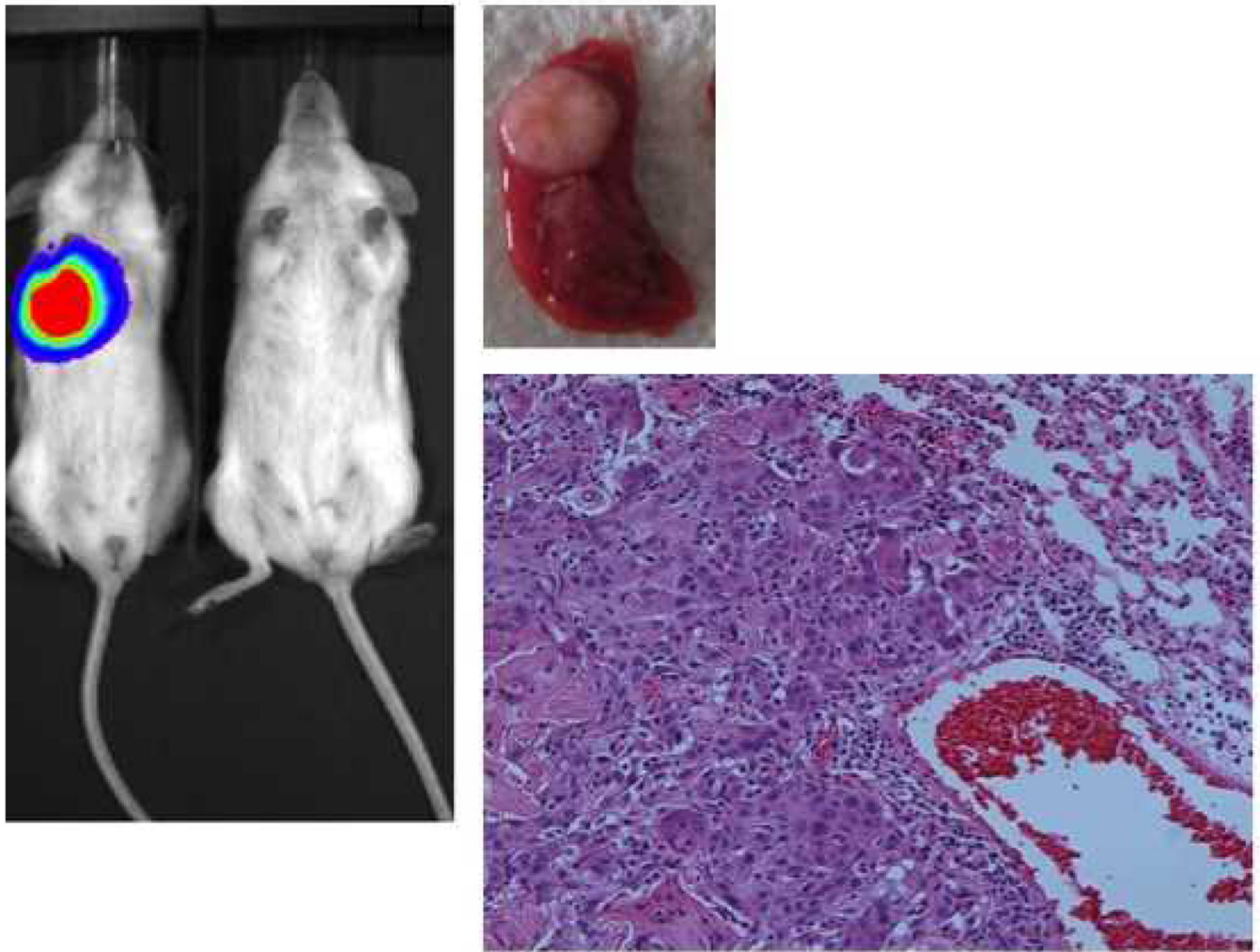
Figure 7.
BMI-1 expression of the fractions of UM-SCC-103. Bands from CD44 fractions (top) and expression of ALDH fractions (bottom).
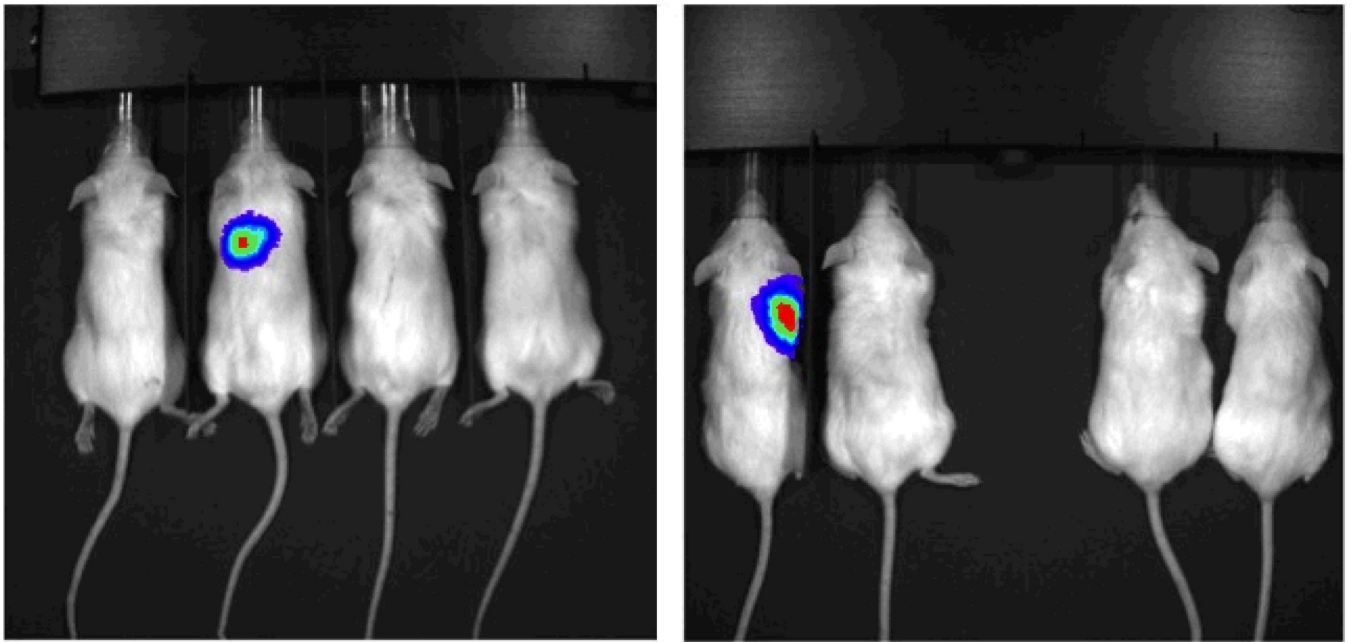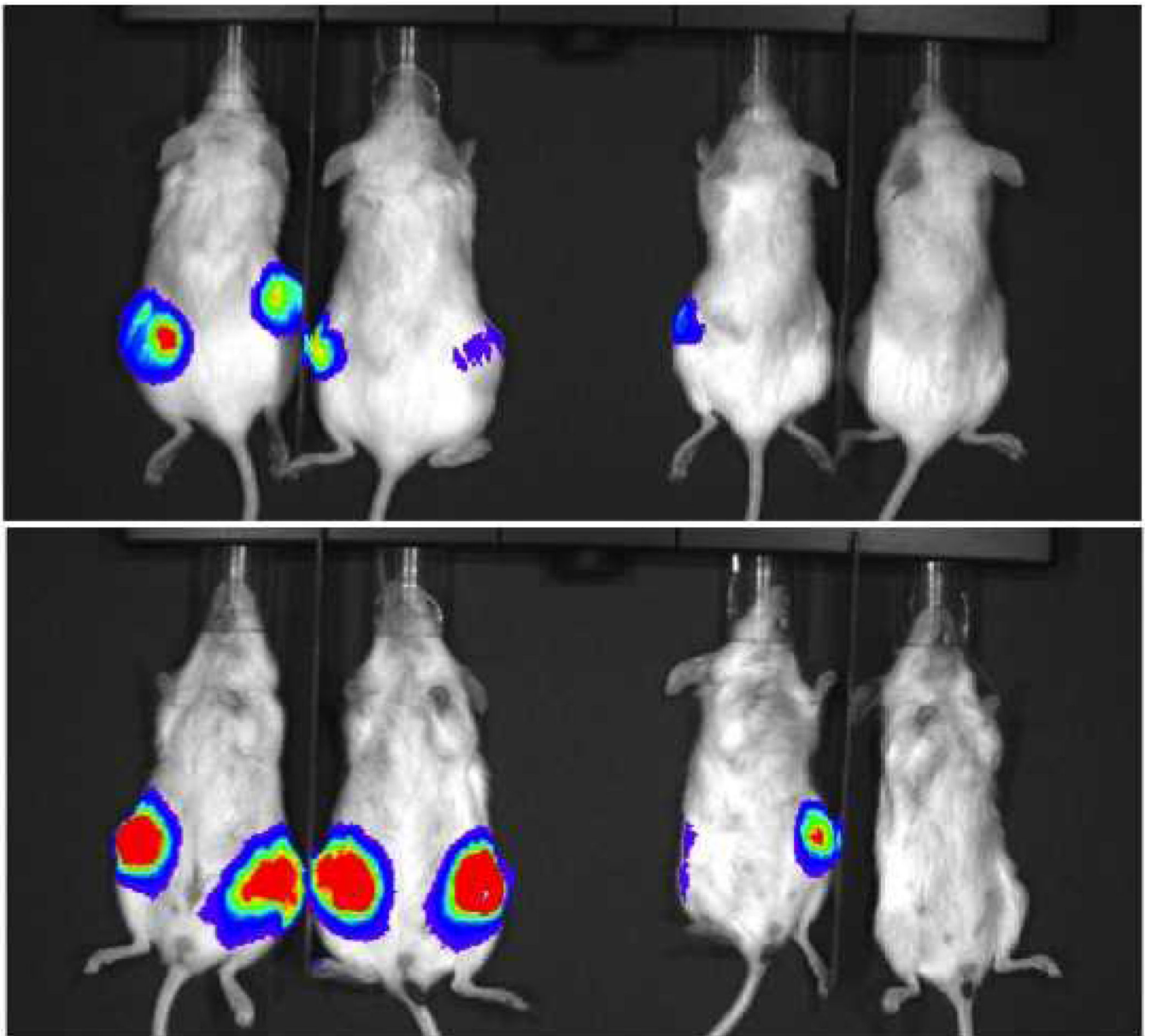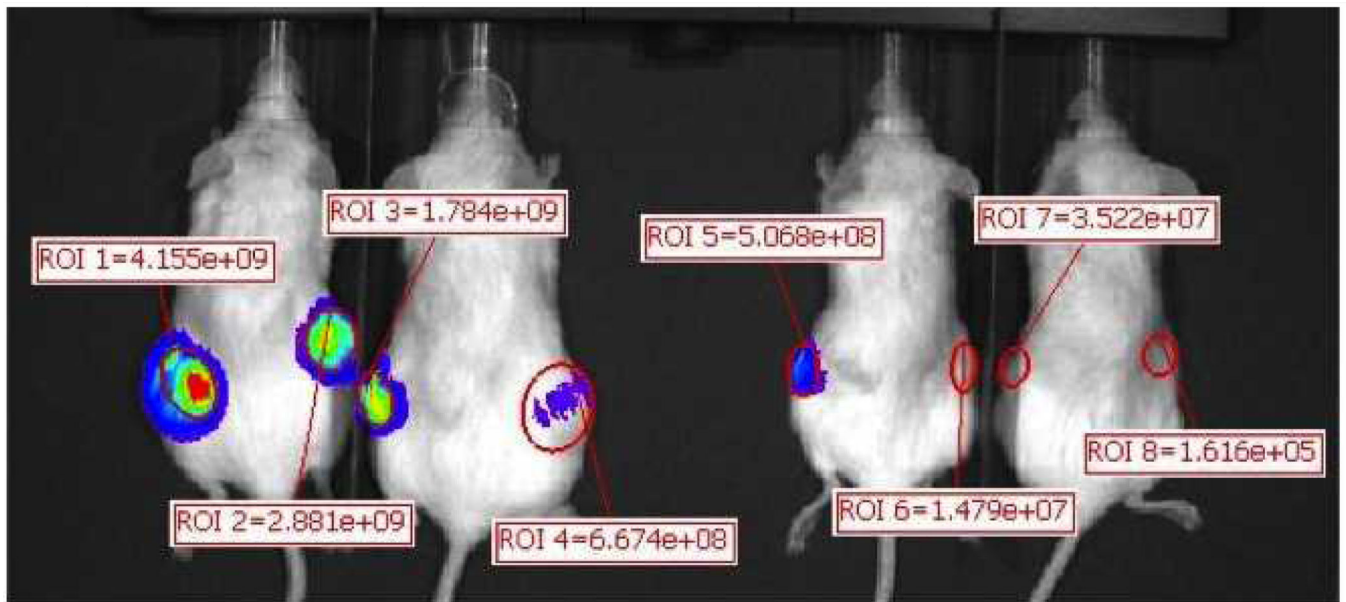
Figure 8.
UM-SCC-103-Luc cells were injected in the tail vein for imaging. Two groups were injected (100,000 cells in the image on the left; 50,000 cells in the image on the right). Two mice were injected with CD44^{high} cells (left) and two mice were injected with CD44^{low} cells (right) in each group. In total, 2/4 mice with CD44^{high} injections developed growth in the lungs, and 0/4 mice with CD44^{low} injections developed tumor growth.

Figure 9.
Tumor was confirmed in the lung of the CD44^{high} 50,000 cell injection by H&E slide.

Figure 10.
Flank growths developed in 4/4 injections from ALDH^{high} cells (left), and only 2/4 injections from ALDH^{low} cells (right).

Figure 11.
Regions were created around each flank injection to determine the radiance of each site for statistical comparison. The ALDH^{high} flank injections had over a ten-fold increase in radiance, on average, when compared with the ALDH^{low} flank injections (Table 2).

Table 1

Lung colonies grew in 2/2 CD44^{high} treatments. After six months, a large abdominal growth was present in the CD44^{high} treatment. There were no results in the CD44^{low} treatments.

Treatment	Euthanized	Lung colonies
HN111 CD44^{high} 100,000 cell tail vein injection	Three months	Yes
HN111 CD44^{high} 100,000 cell tail vein injection	Six months	Yes, tumor in abdomen
HN111 CD44^{low} 100,000 cell tail vein injection	Three months	No
HN111 CD44^{low} 100,000 cell tail vein injection	Six months	No

Table 2

Image Number	ROI	Image Layer	Total Flux [p/s]	Avg Radiance [p/s/cm^2/sr]	Stdev Radiance	Min Radiance	Max Radiance
CD44^{high} flank 1	ROI 1	Overlay	4.16E+09	3.26E+08	1.71E+08	9.92E+07	7.01E+08
CD44^{high} flank 2	ROI 2	Overlay	2.88E+09	2.46E+08	9.44E+07	8.04E+07	4.87E+08
CD44^{high} flank 3	ROI 3	Overlay	1.78E+09	2.77E+08	1.26E+08	1.52E+07	5.66E+08
CD44^{high} flank 4	ROI 4	Overlay	6.67E+08	3.05E+07	9.42E+06	7.74E+06	6.61E+07
CD44^{low} flank 1	ROI 5	Overlay	5.07E+08	8.75E+07	4.16E+07	7.37E+06	2.10E+08
CD44^{low} flank 2	ROI 6	Overlay	1.48E+07	3.42E+06	1.32E+06	8.51E+05	7.14E+06
CD44^{low} flank 3	ROI 7	Overlay	3.52E+07	9.12E+06	4.07E+06	7.53E+05	1.78E+07
CD44^{low} flank 4	ROI 8	Overlay	1.62E+05	3.53E+04	1.02E+05	−2.27E+05	3.67E+05
CD44^{high} flank average			2.37E+09	2.20E+08	1.00E+08	5.06E+07	4.55E+08
CD44^{low} flank average			1.39E+08	2.50E+07	1.18E+07	2.19E+06	5.88E+07